Characteristic Studies on Dealumination of Faujasite-type Zeolite

Kazuo TSUTSUMI, Hisao KAJIWARA, and Hiroshi TAKAHASHI

Institute of Industrial Science, The University of Tokyo, Roppongi, Minato-ku, Tokyo 106

(Received July 11, 1973)

Aluminium ion was extracted stoichiometrically from the framework of the faujasite-type zeolite by EDTA treatment. Dealuminated zeolites with various silica/alumina ratios (from 4.80 to 10.29) were obtained. A dealuminated zeolite does not necessarily show the molecular-sieve-type adsorption isotherm of nitrogen. The lattice constant of zeolite decreases with the silica/alumina ratio. The zeolite with an increased silica/alumina ratio has a higher catalytic activity for a cumene-cracking reaction than the parent H-$Y_{4.80}$ zeolite. It is suggested, on the basis of infrared spectroscopic and calorimetric measurements, that the total number of acid sites decreases with dealumination, while the number of strong acid sites increases. These strong aicd sites seem to contribute to the catalytic activity of dealuminated zeolite.

The catalytic properties of zeolite depend mostly on the type of zeolite, the kind and degree of the exchanged cation, and the silica/alumina ratio. The first three factors have been reported on by many authors, but the effect of the silica/alumina ratio has scarcely been investigated at all. Ward showed that the Brönsted acidity of Ca- or Mg- exchanged faujasite-type zeolite and the catalytic activity for the isomerization of *o*-xylene increased[1] with the silica/alumina ratio.

We have investigated the acidity,[2] and catalytic activity for cumene cracking[3] and the electrostatic-field strength[4] of faujasite-type zeolite as functions of the silica/alumina ratio. In the case of Ca-exchanged zeolite, the electrostatic-field becomes stronger with the increase in the silica/alumina ratio. The cumene-cracking activity of Ca-form zeolite follows in magnitude the change in the electrostatic-field strength. The number of acid sites and the catalytic activity of decationated zeolite increase with the increase in the silica/alumina ratio.

It has been established that the aluminium ion can be readily extracted from the framework of clinoptilolite[5] or erionite[6] by a mineral-acid treatment. The removal of aluminium from mordenite frameworks can also be performed by hydrochloric-acid treatment without distroying the crystal structure as far as the X-ray diffraction patterns are concerned. The catalytic activity and other physicochemical properties of Al-deficient mordenite have been examined by several authors in order to make clear the effect of the dealumination on the diffusion behavior of reactants.[7,8]

It was recently reported that aluminium could also be removed from faujasite-type zeolite frameworks by ethylenediamine-tetraacetic acid (H_4EDTA) treatment.[9] Topchieva and T'huoang reported that the highest activity was exhibited by a specimen in which half of the aluminium atoms had been removed from the faujasite frameworks.[10] Beaumont and Barthomeuf[11–13] and Beaumont *et al.*[14] measured the acidity of the dealuminated zeolite by means of *n*-butylamine titration and infrared spectroscopy.

This paper reports on studies of the effect of the silica/alumina ratio in correlation with the structure, adsorption, acidity, acid strength and catalytic activity, by using the EDTA-treated faujasite-type zeolites.

Experimental

Synthetic sodium faujasite (Linde SK-40) was used as the starting material. The ion exchange for the ammonium ion was performed in an aqueous solution of ammonium chloride by the conventional method. Twenty grams of NH_4^+-exchanged zeolite was treated with an EDTA aqueous solution of an appropriate concentration by means of a Soxhlet extractor. The samples obtained were washed, dried and then equilibrated with saturated vapor of water and the compositions were determined by chemical analysis.

The X-ray powder diagrams were recorded with an X-ray diffractometer (Rigaku Denki Co., Ltd., D–9C Type) using Cu$K\alpha$ radiation, the scanning speed being 1° or 1/8° 2θ/min, the time constant 4 s, receiving slit 0.15 mm, and angular aperture 1°. Silicon was used as an internal standard for the measurement of the lattice constant. The (642) diffraction line of zeolite was used for the measurement.

Mid-infrared spectroscopy has been applied to changes in the zeolite structure with dealumination. The spectra were obtained using the KBr wafer technique. The wafer concentrations were adjusted to obtain the desired absorbance. The spectra were recorded with a Hitachi Model EPI-G3 spectrophotometer.

The nitrogen adsorption isotherms were obtained with a conventional volumetric adsorption apparatus. The pore distribution was calculated by the Inkley method.

The catalytic activity for the cumene-cracking reaction was measured by means of a pulse reactor. The apparatus has been described in detail.[3]

The second infrared spectroscopic technique was used to measure the spectra in the OH stretching region and those of the adsorbed pyridine. The zeolite samples were pressed into a wafer with a thickness of about 10 mg/cm^2. The sample was set in a quartz cell fitted with NaCl windows and heated to 450 °C under 10^{-5} mmHg. The cell was then cooled to room temperature under vacuum; the spectrum was thus obtained. The spectrum of the pyridine adsorbed was also observed. Excess pyridine was adsorbed on the sample and allowed to equilibrate for 3 hr. The spectrum of the adsorbate was obtained after the sample-adsorbate had been evacuated at 250 °C in order to remove the physically adsorbed pyridine.

The differential heats of the adsorption of ammonia were measured in order to estimate the acid strength of zeolite. About one gram of zeolite was placed in the stainless-steel cell, and evacuated at 400 °C under 10^{-5} mmHg over a period of several hours. The cell was set in a twin con-

duction-type calorimeter until thermal equilibrium was reached at 25 °C. Gaseous ammonia was then introduced into the cell. The heat liberated was recorded and calibrated by a known amount of heat.

Results and Discussion

Chemical Compositions. The compositions of the samples obtained are shown in Table 1. Zeolite becomes cation-deficient with dealumination. The silica/alumina ratios are plotted against the moles of EDTA used in Fig. 1. The broken line indicates the relation calculated by Eq. (1).

$$x\mathrm{H_4EDTA} + \mathrm{NH_4AlO_2(SiO_2)_{2.40}} \longrightarrow x\mathrm{NH_4AlEDTA} + (\mathrm{NH_4AlO_2})_{1-x}(\mathrm{H_2O})_{2x}(\mathrm{SiO_2})_{2.40} \quad (1)$$

The close fit of the points shows that the dealumination reaction proceeds stoichiometrically as Kerr suggested.[9]

Table 1. Zeolite compositions

Sample	Composition
H-$Y_{4.80}$	$0.78(NH_4)_2O\cdot 0.15Na_2O\cdot Al_2O_3\cdot 4.80SiO_2$
H-$Y_{5.97}$	$0.71(NH_4)_2O\cdot 0.17Na_2O\cdot Al_2O_3\cdot 5.97SiO_2$
H-$Y_{6.54}$	$0.70(NH_4)_2O\cdot 0.18Na_2O\cdot Al_2O_3\cdot 6.54SiO_2$
H-$Y_{7.38}$	$0.68(NH_4)_2O\cdot 0.19Na_2O\cdot Al_2O_3\cdot 7.38SiO_2$
H-$Y_{10.29}$	$0.67(NH_4)_2O\cdot 0.16Na_2O\cdot Al_2O_3\cdot 10.29SiO_2$

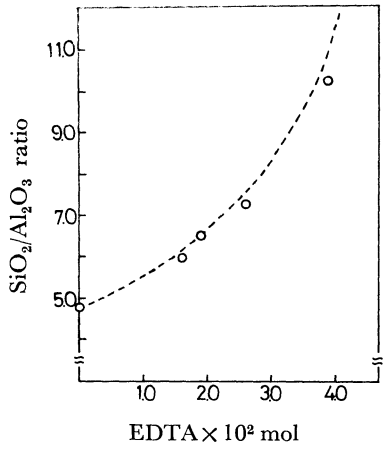

Fig. 1. Correlation between silica/alumina ratio of zeolites and the moles of EDTA added.
----: Calcd

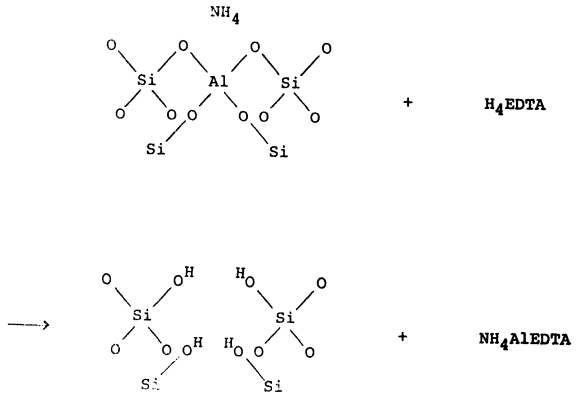

Fig. 2. Two-dimentional representation of the dealuminated zeolite.

The resulting model of zeolite when aluminium ion was removed from the framework according to Eq. (1) is illustrated two-dimensionally in Fig. 2.

Structural Characters. The X-ray diffraction diagrams are illustrated in Fig. 3. It can be seen that the structure of zeolite is not essentially destroyed by the treatment with EDTA. However, on the basis of the changes in the half-value of the breadth and integral intensity, amorphous species were partially produced as EDTA treatment became severe.

The correlation between the lattice constant and the silica/alumina ratio is plotted in Fig. 4. The lattice is contracted as the silica/alumina ratio becomes higher, which seems to be due to the removal of the constitutional aluminium of the zeolite lattice. It is well-known that the lattice constant decreases with the increase in the silica/alumina ratio in X- and Y-type zeolites.[15–17] The results obtained are of interest in the light of this fact.

The mid-infrared spectra of H-$Y_{4.80}$, H-$Y_{7.38}$ and H-$Y_{10.29}$ are shown in Fig. 5. The absorption bands were assigned in detail by Flanigen and Khatami.[18]

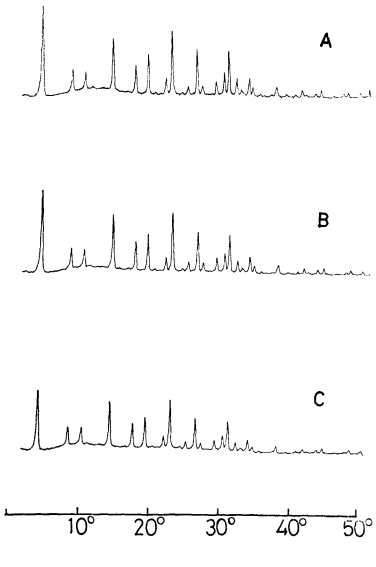

Fig. 3. X-Ray diffraction patterns of zeolites.
A: H-$Y_{4.80}$, B: H-$Y_{7.38}$, C: H-$Y_{10.29}$

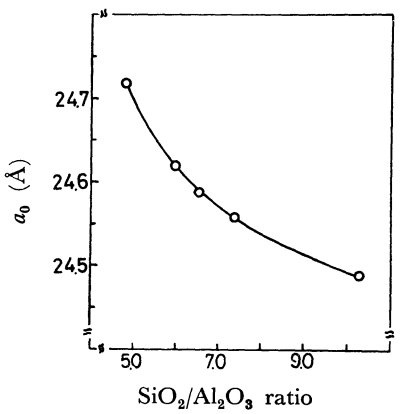

Fig. 4. Correlation between silica/alumina ratio of zeolites and lattice constant.

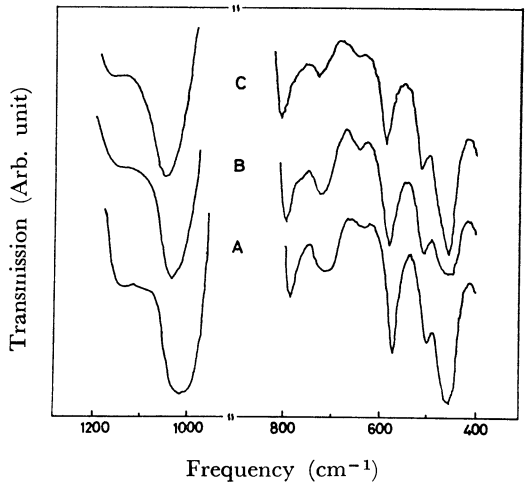

Fig. 5. Mid-infrared spectra of zeolite.
A: H-$Y_{4.80}$, B: H-$Y_{7.38}$, C: H-$Y_{10.29}$

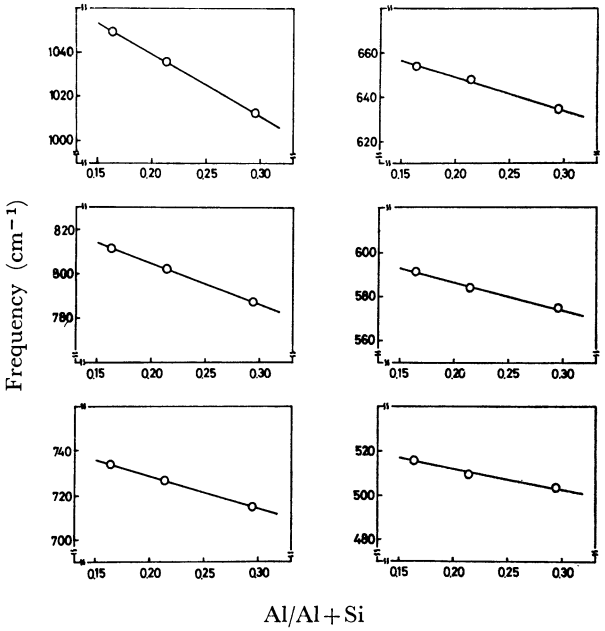

Fig. 6. Correlations between silica/alumina ratio and frequency of various adsorption bands.

Except for the band at about 460 cm^{-1}, the bands are shifted to higher frequency with an increase in the silica/alumina ratio.[19,20] The most intense absorption band, caused by the T–O (T represents Si or Al) asymmetric stretching vibration in the 1010—1050 cm^{-1} region, is very sensitive to the silica/alumina ratio. The absorption wave numbers change linearly with the Al fraction in the zeolite frameworks as is shown in Fig. 6. Since the masses of Al and Si are similar, the increase in frequency with the decrease in Al content is due to the difference in bond length and bond order. The fact that the bond length of Al–O is longer and Al is more electronegative seems to cause a decrease in the force constant of the T–O bond.

Nitrogen Adsorption Behaviors. N_2 adsorption isotherms at the temperature of liquid nitrogen are shown in Fig. 7. H-$Y_{4.80}$ shows a typical molecular-sieve adsorption isotherm; H-$Y_{7.38}$ and H-$Y_{10.29}$ samples with

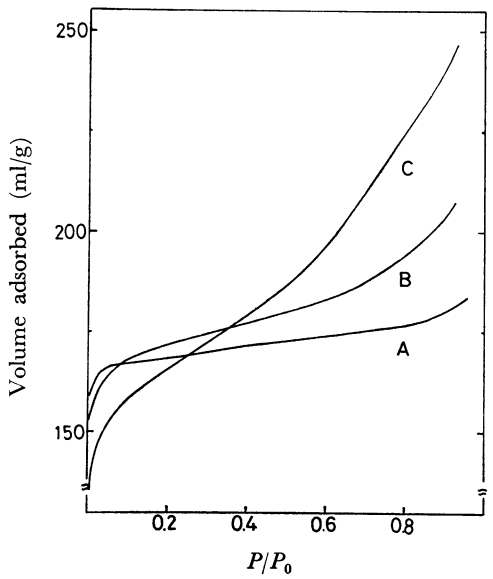

Fig. 7. Nitrogen adsorption isotherms.
A: H-$Y_{4.80}$, B: H-$Y_{7.38}$, C: H-$Y_{10.29}$

higher silica/alumina ratios adsorb increased amounts of nitrogen at higher relative pressures. This is probably due to the presence of amorphous parts. The cumulative pore volume distributions calculated from the adsorption isotherm show that, as the silica/alumina ratio increases, the pore size becomes widely distributed and the typical regular pore structure of zeolite must be partially destroyed.

Catalytic and Acid Properties. Figure 8 shows the cracking activity *vs.* silica/alumina ratio. With the rise in silica/alumina ratio the activity increases reaching a maximum and then decreases. Since Brönsted acid sites are effective for a cumene-cracking reaction, the increased activity seems to be due to the change in the surface-acid properties.

The infrared spectra and the heat of adsorption were studied in order to estimate the acidity and the acid strength.

Hydroxyl bands were detected on H-$Y_{4.80}$ zeolite near 3640 and 3550 cm^{-1} after evacuation at 450 °C.[21] Both hydroxyl groups are known to be acidic. An additional band was observed at 3750 cm^{-1} in the case of Al-deficient zeolite. The band agrees with that of the isolated silanol on the silica surface.[22]

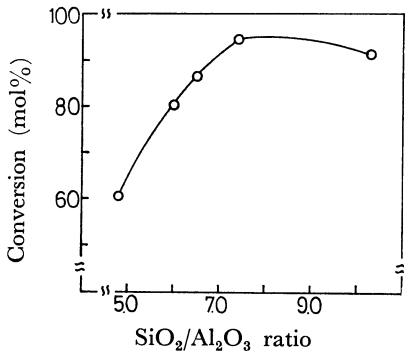

Fig. 8. Correlation between silica/alumina ratio and cumene-cracking activity.
Pretreatment, 550 °C; Reaction, 300 °C

Since four Si–OH bonds are expected to be newly formed by treatment with EDTA, it is probable that the additional band appears at 3750 cm^{-1} (Fig. 2).

Under pyridine adsorption, all the hydroxyl bands were eliminated and new bands were detected at 1400—1700 cm^{-1}. The integrated adsorptivities were measured for the 1540 cm^{-1} band, which was assigned to the pyridinium ion bonded to the Brönsted acid site.[21] From the adsorptivities, the Brönsted acid site was calculated using the apparent integrated molar adsorption intensity of 2.5 cm/μmol.[23] The results are shown in Table 2 for H-$Y_{4.80}$, H-$Y_{7.38}$, and H.$Y_{10.29}$ zeolite. The order of the number of acid sites is H-$Y_{7.38}$>H-$Y_{4.80}$>H-$Y_{10.29}$. Since the protonic acid site is combined with a zeolite negative site, that is $(AlO_2)^-$ ion, Brönsted acid sites are considered to decrease in proportion to dealumination. However, H-$Y_{7.38}$ zeolite showed an increased acidity. This can be explained as follows. The proton becomes mobile as the negative shield of the structural aluminium ion is decreased. As a result, an increased number of sites become effective for the acid. The ratio of Brönsted sites to Lewis sites was also calculated from the integrated absorptivities of the 1490 cm^{-1} band. The ratio of $\varepsilon^{B}_{1490}/\varepsilon^{L}_{1490}$ is assumed to be 5.2.[24] The ratio increases with the silica/alumina ratio. This results from the fact that the distance between Brönsted acid sites becomes longer as Al is removed, and the conversion of the Brönsted sites into Lewis sites on dehydroxylation becomes unfavorable. The H-$Y_{10.29}$ zeolite shows a higher cracking activity than would be expected from its acidity, suggesting the contribution of acid strength to be significant.

Table 2. Brönsted and Lewis acid site concentrations measured by the infrared spectra of adsorbed pyridine

Sample	log $[T_0/T]d\nu$[a] (cm^{-1})	B acid[b] (mmol/g)	B/L
H-$Y_{4.80}$	8.9	0.44	0.9
H-$Y_{7.38}$	10.8	0.66	5.8
H-$Y_{10.29}$	3.3	0.18	10.2

a) 1540 cm^{-1} band of adsorbed pyridine. b) Apparent integrated molar adsorption intensity taken as 2.5 cm/μmol.

The effects of dealumination on the strength and distribution of acid sites were investigated by measuring the differential heats of adsorption of ammonia. The differential heats of adsorption are plotted against the ammonia molecules adsorbed in Fig. 9. The region of initial adsorption seems to be important in interpreting the relation between the energy distribution and the activity. The initial heats on the samples used are all over 25 kcal/mol at the adsorbed amount of 3×10^{-2} mmol/g. If we assume that one ammonia molecule is adsorbed on each acid site, the number of acid sites with a heat of adsorption of ammonia of over 23 kcal/mol is larger in H-$Y_{10.29}$ than in others. As the amount adsorbed increases to about 1.75 mmol/g, heats of adsorption on H-$Y_{10.29}$ and H-$Y_{7.38}$ fall off steeply to about 14 kcal/mol; on the other hand, the

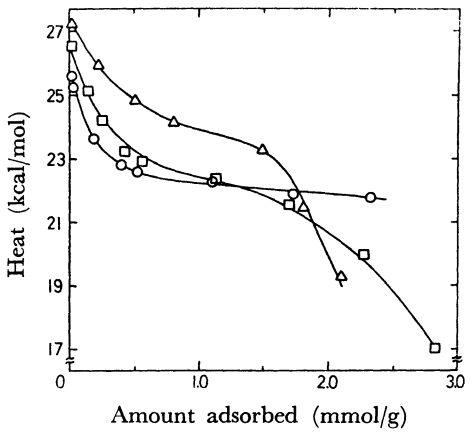

Fig. 9. Differential heats of adsorption of ammonia at 25 °C.
—○—: H-$Y_{4.80}$, —□—: H-$Y_{7.38}$, —△—: H-$Y_{10.29}$

heats of adsorption on H-$Y_{4.80}$ decrease gradually. As a result, the total number of acid sites with heats of adsorption of over 20 kcal/mol of H-$Y_{4.80}$ is larger than that of H-$Y_{10.29}$ and H-$Y_{7.38}$. This would not contradict the infrared spectroscopic data, since the heat of adsorption of ammonia would depend on both Brönsted and Lewis acids and the conversion of the former into the latter could easily occur on H-$Y_{4.80}$.

It is thus evident that the ratio of strong acid sites to all sites increases with dealumination. Beaumont *et al.* showed by means of infrared spectroscopy that the concentration of weak acid sites was lower in aluminium-deficient zeolite than in Y zeolite, while the concentration of strong acid sites was higher.[14] The results agree with ours. The strong acid sites thus formed seem to produce the higher cracking activity of H-$Y_{10.29}$, though the pyridinium-ion concentration of H-$Y_{10.29}$ is lower than that of H-$Y_{4.80}$.

It can be concluded that the change in acid properties with dealumination predominantly influences catalytic activity for the cumene-cracking reaction. However, the appearance of amorphous parts might play a role in the catalytic activity, especially in the case of H-$Y_{10.29}$. The effect of the pore volume on catalytic activity seems to be significant in the structure-sensitive reaction.

References

1) J. W. Ward, *J. Catal.*, **17**, 355 (1970).
2) M. Ikemoto, K. Tsutsumi, and H. Takahashi, This Bulletin, **45**, 1330 (1972).
3) K. Tsutsumi and H. Takahashi, *J. Catal.*, **24**, 1 (1972).
4) K. Tsutsumi and H. Takahashi, *J. Phys. Chem.*, **76**, 110 (1972).
5) R. M. Barrer and M. B. Makki, *Can. J. Chem.*, **42**, 1481 (1964).
6) S. P. Zhdanov and B. G. Novikov, *Dokl. Akad. Nauk. S. S. S. R.*, **166**, 1107 (1966).
7) P. E. Eberly, Jr., C. N. Kimberlin, Jr., and A. Voorhies, Jr., *J. Catal.*, **22**, 419 (1971).
8) W. L. Kranich, Y. H. Ma, L. B. Sand, A. H. Weiss, and I. Zwiebel, "Molecular Sieve Zeolite-I," (R. F. Gould, ed.), p. 502, Adv. Chem. Ser.-101, (1971).

9) G. T. Kerr, *J. Phys. Chem.*, **72**, 2594 (1968).
10) K. V. Topchieva and H. S. T'houang, *Kinet. Katal.*, **11**, 490 (1970).
11) R. Beaumont and D. Barthomeuf, *C. R. Acad. Sc. Paris, Ser. C.*, **1971**, 363.
12) R. Beaumont and D. Barthomeuf, *J. Catal.*, **26**, 218 (1972).
13) R. Beaumont and D. Barthomeuf, *ibid.*, **27**, 45 (1972).
14) R. Beaumont, P. Pichat, D. Barthomeuf, and Y. Trambouze, Prep. 5th Int. Cong. Catal., Miami (1972).
15) A. C. Wright, J. P. Rupert, and W. T. Granquist, *Amer. Mineral.*, **53**, 1293 (1968); **54**, 1484 (1969).
16) E. Dempsey, G. H. Kuhl, and D. H. Olson, *J. Phys. Chem.*, **73**, 387 (1969).
17) J. V. Smith, "Molecular Sieve Zeolite-I," (R. F. Gould, ed.), p. 171, Adv. Chem. Ser.-101, (1971).
18) E. M. Flanigen and H. Khatami, *ibid.*, p. 201.
19) P. Pichat, R. Beaumont, and D. Barthomeuf, *C. R. Acad. Sci., Paris, Ser. C*, 612 (1971).
20) O. L. Šarc, *J. Phys. Chem.*, **75**, 2408 (1971).
21) For example, J. M. Ward, *J. Catal.*, **9**, 225 (1967).
22) For example, R. S. McDonald, *J. Phys. Chem.*, **62**, 1168 (1958).
23) Y. Watanabe and H. W. Habgood, *ibid.*, **72**, 3066 (1968).
24) M. Lefrancois and G. Malbois, *J. Catal.*, **20**, 350 (1971).